Separation and Purification Technology 172 (2017) 350–356

Contents lists available at ScienceDirect

Separation and Purification Technology

journal homepage: www.elsevier.com/locate/seppur

Scaling-up of multi-capsule depth filtration systems by modeling flow and pressure distribution

A.U. Krupp [a], C.P. Please [a], A. Kumar [b], I.M. Griffiths [a,*]

[a] Mathematical Institute, Andrew Wiles Building, Woodstock Road, Oxford OX2 6GG, UK
[b] Pall Life Sciences, 20 Walkup Drive, Westborough, MA 01581, USA

ARTICLE INFO

Article history:
Received 28 April 2016
Received in revised form 15 July 2016
Accepted 17 July 2016
Available online 20 July 2016

Keywords:
Scale-up
Modeling
Depth filtration
Filter capacity
Fouling

ABSTRACT

Scaling-up of filtration systems in the pharmaceutical industry to provide the correct filtration capacity is a complex process. When several filters are used in parallel, the pressure and flow distribution within the system can be modeled using well-established constitutive laws to a high degree of accuracy, as shown in this paper. By combining the model with experimental fouling data, it is also possible to accurately predict the flow and pressure distribution during an entire filtration run. A process is discussed that uses this model to determine how the capacity of a filtration system can be accurately predicted using a minimal set of measurements.

1. Introduction

Scaling-up of filtration processes from R&D to production level in the pharmaceutical industry is a complex undertaking with strong implications on the profitability of the corresponding drug development project [1,2]. A key challenge lies in providing the appropriate filtration capacity for production-level batch sizes based on laboratory or testing-plant scale measurements [3]. This can, for example, be achieved by using dimensional analysis to scale-up filters used in the laboratory-scale process [4] or by using several filters of standardized size in parallel [5]. When using filters in parallel, in order to accurately predict the capacity of the entire system it is crucial to understand how the different filters in the system affect each other, because the flow and pressure distribution within the system will not be homogeneous. The individual operating conditions of a given filter, such as the pressure difference across it and its resistance due to clogging, depend not only on conditions imposed from the outside but also on factors such as the filter's position within the system and the resistances of the other filters.

In order to be able to make accurate predictions about a scaled-up system, it is necessary to predict the pressure distribution within a given system of parallel filters. This becomes complicated as the filters clog at different rates during the filtration run due to the inhomogeneous pressure distribution within the system, which in turn changes the pressure distribution and vice versa.

In this paper, we derive a mathematical model for calculating the pressure distribution within a scaled-up system composed of a set of depth filters connected in parallel, termed a *multi-capsule depth filter*. The model is validated using experimental data and used to predict scale-up behavior.

A general approach when considering filter clogging in scaling-up a device is to model the individual membrane fouling using Hermia's laws [6] as in [3,7], which has the advantage of giving insights into the underlying fouling mechanisms. However, this can be a cause for errors if the model's predictions are not accurate or add complexity if several mechanisms have to be considered to model the fouling accurately [8,9]. Here we describe how to combine experimental data from the clogging of a single capsule with our model to accurately predict the pressure distribution within a multi-capsule depth filter during an entire filtration run. Our method has the advantage of not requiring knowledge about the underlying clogging mechanisms since all relevant information is provided by the experimental data.

1.1. Multi-capsule depth filtration

By depth filtration we denote the filtration process where the feed flows into and not along the membrane, commonly described as a normal flow or dead-end configuration, and the filtrate is deposited within the entire depth of the filter and not only at the

* Corresponding author.
E-mail address: ian.griffiths@maths.ox.ac.uk (I.M. Griffiths).

http://dx.doi.org/10.1016/j.seppur.2016.07.028
1383-5866/

surface [10]. In the pharmaceutical industry, depth filtration is typically used to clarify process streams before a final sterile filtration [11,12]. In order to process the feed from industrial-sized bioreactors (>2000 L), a depth filter with a sufficiently large surface area is required, which is in general achieved by using several depth filters of some standardized size in parallel [13]. Typical depth filters are housed in disc-shaped capsules, which in turn are then connected in parallel and stacked on top of each other, principally to reduce the footprint of the filtration system, though other operational considerations may also play a role. It is such a stack of depth-filter capsules that we refer to as a multi-capsule depth filter.

The inlet to the multi-capsule depth filter is usually located at the bottom of the device, while the outlet can be positioned either at the bottom or the top. If the outlet is located at the bottom, the feed flows upwards while the filtrate flows downwards, hence it is called a *counter-current* configuration. If the outlet is located at the top, both the filtrate and feed flow upwards and it is called a *co-current* configuration.

Given that full-scale experiments on multi-capsule depth filters are very costly, the dimensions of production-level multi-capsule depth filters must be calculated using safety margins. By comparing the predictions from our model with experimental data, we will show how our model can describe the pressure distribution within a multi-capsule depth filter to determine the used capacity of a depth filter and thus significantly reduce the required safety margins. Moreover, we will see that the parameters from our model can be used to predict the pressure distribution within multi-capsule depth filters with an arbitrary number of capsules. We will also show how using clogging data from experiments to simulate filtration runs leads to high-accuracy predictions.

2. Mathematical model

We consider schematic set-ups for the co-current and counter-current configuration with N capsules as in Fig. 1. The inlets and outlets of the capsules are connected in series, hence at a given inlet the fluid can either pass through the depth filter or move to the next capsule. Once the fluid has passed through a filter, it flows through the connecting pipes to the outlet of the entire device.

The pressure at the inlet is denoted by P_{in} and at the outlet by P_{out}. For capsule i, $1 \leqslant i \leqslant N$, we denote the pressure at the inlet by $P_{i,\text{in}}$ and at the outlet by $P_{i,\text{out}}$. The flux through capsule i is denoted by Q_i, and the total flux through the system by $\mathcal{Q}$. We denote the height difference of capsule i relative to the inlet by h_i.

2.1. Constitutive relationships between fluid flow and pressure differences

We assume that the pressure in the system is composed of a hydrostatic and hydrodynamic part only. The inlet and outlet pressures $P_{i,\text{in}}$ and $P_{i,\text{out}}$ can be reduced to their hydrodynamic part only by setting

$$\widetilde{P}_{i,\text{in}} = P_{i,\text{in}} - \rho g h_i \text{ and } \widetilde{P}_{i,\text{out}} = P_{i,\text{out}} - \rho g h_i, \tag{1}$$

where ρ denotes the density of the liquid and g the gravitational acceleration. In the following, we need only work with the hydrodynamic pressures, $\widetilde{P}$, even if the capsules are stacked on top of each other or are located at different heights; we will drop the tilde in order to facilitate reading.

For practical filter operating regimes, the constitutive relation between the pressure difference, ΔP_i, across and the flow Q_i through the i^{th} filter is approximated well by Darcy's law

$$Q_i = -\frac{k_i A_i}{\eta L_i} \Delta P_i, \tag{2}$$

where A_i denotes the surface area, k_i the permeability and L_i the depth of the filter, and η denotes the dynamic viscosity of the liquid. We will abbreviate (2) by $Q_i = \alpha_i \Delta P_i$, where $\alpha_i = -k_i A_i / \eta L_i$ is the *Darcy parameter* of capsule i.

We assume laminar flow in the connecting pipes between two capsules as the relevant Reynolds number for the flow is of order 10^{-1} (using data[1]), hence, motivated by Poiseuille flow, we use a constitutive relation of the form

$$Q = r \Delta P, \tag{3}$$

where r depends on characteristics of the connecting pipes only. We will denote the parameter r of the connecting pipes between capsule i and $i+1$ by $r_{i,\text{in}}$ at the inlet and by $r_{i,\text{out}}$ at the outlet. The resistance between the inlet and the first capsule is denoted by r_{in} and the resistance between the outlet and the connecting capsule by r_{out}.

From an operational perspective, we require that the fluid occupies the entire device so that the fluid does not cavitate. Hence the pressures at the inlet and outlet must equal at least the hydrostatic pressure of the fluid in the device. For both set-ups we therefore require

$$P_{\text{in}} \geqslant \rho g \cdot \max\{h_1, \ldots, h_N\} \tag{4}$$

and for the counter-current configuration, we also require the same inequality to hold for P_{out}.

2.2. Derivation of the system of linear equations describing the pressure distribution and fluid flow within the multi-capsule depth filter

Darcy's law (2) and the Poiseuille relation (3) can be combined to form a system of linear equations for the inlet and outlet pressures $P_{i,\text{in}}$ and $P_{i,\text{out}}$, $1 \leqslant i \leqslant N$; knowing these will also allow us to calculate the flow distribution. The governing equations for the inlets of the capsules are then given for $i = 1, \ldots, N-1$ by

$$r_{i,\text{in}}(P_{i,\text{in}} - P_{i+1,\text{in}}) = \sum_{l=i+1}^{N} Q_l \tag{5}$$

and

$$r_{\text{in}}(P_{\text{in}} - P_{1,\text{in}}) = \mathcal{Q} \tag{6}$$

for the inlet of the device.

Regarding the governing equations for the outlets of the capsules, we must distinguish between co-current and counter-current configuration. In the co-current configuration we have for $i = 1, \ldots, N-1$

$$r_{i,\text{out}}(P_{i,\text{out}} - P_{i+1,\text{out}}) = \sum_{l=1}^{i} Q_l \tag{7}$$

and

$$r_{\text{out}}(P_{N,\text{out}} - P_{\text{out}}) = \mathcal{Q} \tag{8}$$

at the outlet. For the counter-current configuration we have for $i = 1, \ldots, N-1$

$$r_{i,\text{out}}(P_{i+1,\text{out}} - P_{i,\text{out}}) = \sum_{l=i+1}^{N} Q_l \tag{9}$$

and

$$r_{\text{out}}(P_{1,\text{out}} - P_{\text{out}}) = \mathcal{Q} \tag{10}$$

[1] The kinematic viscosity ν is $\nu \approx 10^{-6}$ m^2/s, the length scale between the filter and the filter capsule is of order 10^{-2} m, the velocity is of order 10^{-3} m/s and the aspect ratio between for the length is of order 10^{-2}.

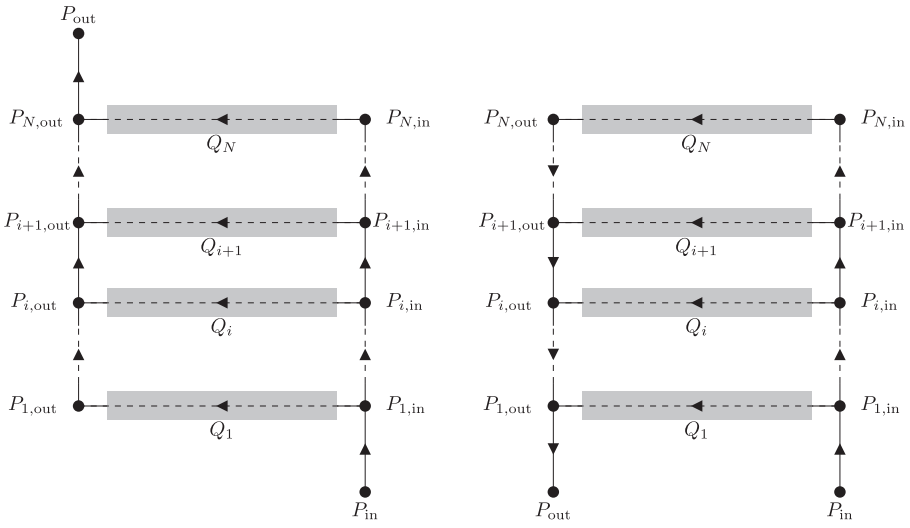

(a) Co-current configuration (b) Counter-current configuration

Fig. 1. Schematic of a multi-capsule depth filter in co-current (left) and counter-current (right) configuration. Each capsule is represented by a horizontal line, with the shaded rectangles representing the depth filters. The fluid enters the device at the inlet, marked by P_{in}, and leaves it at the outlet, marked by P_{out}.

at the outlet. Darcy's law (2) reads as

$$\alpha_i(P_{i,\text{in}} - P_{i,\text{out}}) = Q_i \tag{11}$$

for $i = 1, \ldots, N$ and we have conservation of flux

$$\sum_{i=1}^{N} Q_i = \mathcal{Q}. \tag{12}$$

We can use (11) to replace each Q_i in the set of Eqs. (5)–(10), to give $2N$ equations for $2N + 2$ unknowns. Specifying two of the three parameters P_{out}, P_{in} or $\mathcal{Q}$ via a combination of Eqs. (11) and (12) results in a linear system with $2N$ equations for $2N$ unknowns for which a unique solution exists (see Appendix A for details).

2.3. Simulating an entire filtration run

During a filtration run, fouling will change the permeability of the capsules. Given that the flow distribution is in general non-uniform within a multi-capsule depth filter, the permeabilities of the different capsules will decrease at different rates during the filtration run, which in return changes the flow and pressure distribution. To model this evolution over time, we assume that the permeability k_i of capsule i, and thus its Darcy parameter α_i, at a given time t depend only on the throughput V_i^t, that is, the total volume of fluid processed by capsule i up to time t, and that this relationship is sufficiently smooth.

To simulate the filtration run, we use an explicit Euler-scheme with constant (small) timestep Δt. At each time t, we compute the pressure distribution by solving the linear system described by Eqs. (5)–(10) with corresponding Darcy constants $\alpha_1^t, \ldots, \alpha_N^t$. The total throughput $V_i^{t+\Delta t}$ through capsule i at time $t + \Delta t$ is then computed by

$$V_i^{t+\Delta t} = V_i^t + \Delta t\ \alpha_i^t\ (P_{i,\text{out}} - P_{i,\text{in}}). \tag{13}$$

The Darcy parameter of capsule i at time $t + \Delta t$, $\alpha_i^{t+\Delta t}$, can then be computed by

$$\alpha_i^{t+\Delta t} = \alpha(V_i^{t+\Delta t}), \tag{14}$$

where the α–V relationship is given either by some function in closed form or using experimental data as described in Section 3.2.1.

We repeat the entire process until some final condition, for example, $P_{\text{in}} - P_{\text{out}}$ exceeds some threshold value, is satisfied.

3. Validation of the mathematical model

In this section, we validate our theory by comparing the predictions of our mathematical model with measurements taken by Collins et al. [5]. Here, clean-water flow tests that do not change the permeability were first conducted to measure the flow and pressure distribution within a multi-capsule depth filter. Following this, full filtration runs with dissolved yeast were conducted to simulate a filtration run with a mammalian cell culture.

3.1. Comparison with clean-water flow tests

In a clean-water flow test, water is supplied at a constant flux as a feed, thus no clogging occurs and so the flow and pressure distribution are constant (after a short start-up transition). In the first set of experiments in [5], clean-water flow tests were conducted with multi-capsule depth filters with five and ten capsules, each in co-current and counter-current configuration. Regarding the experiments with five capsules, the authors measured the pressure at the inlet side of the filters of each capsule and the outlet side of capsules 1 and 5. For the experiments with ten capsules, the authors measured the pressure at the inlet side of the filters 1–5, 7, 9, 10 and the outlet side of capsules 1 and 10. The measurements in each experiment were taken for fluxes of 100, 200 and 300 litres per square meter per hour (LMH).

These experimental values were used to determine the parameters α, r_{in} and r_{out} by assuming the values were the same for each capsule as described in Appendix B. The results for the co-current and counter-current configuration with five capsules are shown in Fig. 2a and the corresponding results for ten capsules are shown in Fig. 2b. As the measured pressures were all around 1 bar, we plot the absolute errors in pressure between the measurements and our predictions. In the figures, the absolute error for the outlet represents the absolute error between the prediction and the measurement for the outlet of the bottom capsule (co-current configuration) or for the outlet of the top capsule (counter-current configuration). We do not plot the error for capsule 1 and the outlet of the system, as their values were used as boundary conditions.

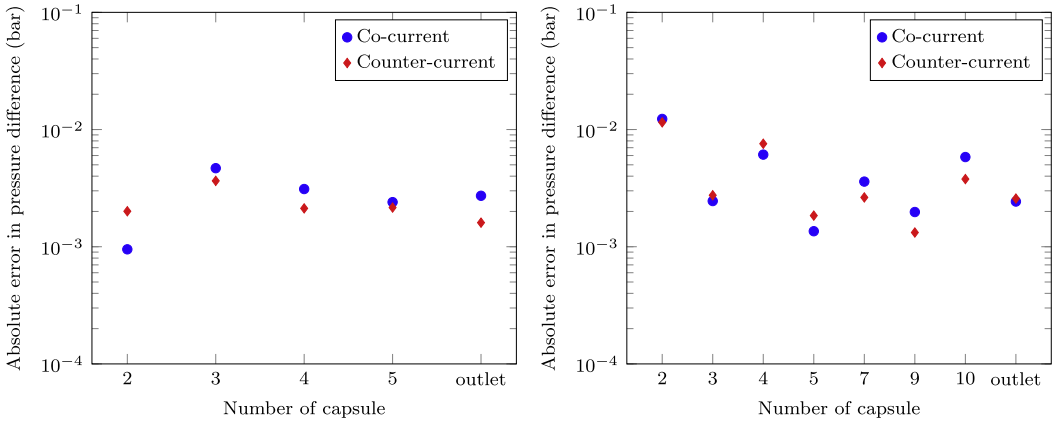

(a) Five-capsule depth filter (b) Ten-capsule depth filter

Fig. 2. Validating the model. We plot the average error between the predicted and measured pressure at each capsule based on clean-water flow tests with 100, 200 and 300 LMH.

The model accurately fits the data with absolute errors being generally in the range of 10^{-3}–10^{-2} bar.

3.2. Comparison with an entire filtration run

In the second set of the experiments, two ten-capsule depth filters, one in co-current and one in counter-current configuration, were challenged with a mixture of homogenized yeast and whole yeast at 300 LMH until a threshold pressure was attained, in order to simulate a filtration run with a mammalian cell culture. In this instance, we expect the depth filters to clog at different rates due to the difference in fluxes and thus for their permeabilities to change at different rates as well, which in turn changes the pressure distribution within the multi-capsule depth filter.

In order to precisely predict the pressure distribution within the multi-capsule depth filter during the filtration run, we have to quantify how the Darcy parameter α changes with throughput V. We first discuss how to obtain the α–V relationship and then use this to compare our predictions against the measurements.

3.2.1. Computing change in permeability due to clogging

To obtain experimental data on the change in permeability due to clogging, a single capsule was challenged with the same mixture of homogenized yeast and whole yeast used for the filtration run at 300 LMH while the differential pressure $\Delta P(V)$ across the capsule, depending on the throughput V, was recorded, see Fig. 3a.

As we assume that the permeability k of a capsule only depends on the throughput V, i.e. $k = k(V)$, we use Darcy's law (2) to infer

$$\alpha(V) = \frac{Q}{\Delta P(V)} \tag{15}$$

where $\alpha(V) = -k(V)A/\eta L$ is the Darcy parameter.

The recorded ΔP–V data for an experiment at constant flux can thus be used to determine $\alpha(V)$, the result for the relative Darcy parameter $\alpha(V)/\alpha(0)$ is shown in Fig. 3b.

As the measurements contain outliers, we apply a smoothing method where we require consecutive measurements to deviate by at most ten percent. This smoothing is depicted by the line in Fig. 3b; the experimental results are depicted by dots. As the measurements were stopped once the threshold differential pressure of 1 bar was surpassed, we extended the function by assuming an exponential decay law. We can use the resulting α–V relationship as a function in numerical methods by linearly interpolating between consecutive measurements.

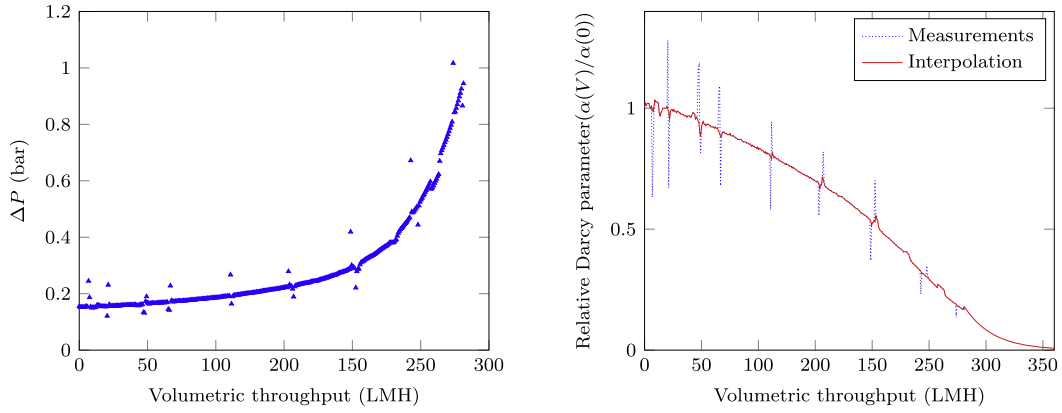

(a) Measured differential pressure when challenging a single capsule with a homogenized/whole-yeast mixture at 300 LMH

(b) Interpolated and normalized Darcy parameter in dependency of the volumetric throughput

Fig. 3. Measurement and interpolation results for the Darcy parameter.

3.2.2. Comparison of predictions and measurements

We combined our model with the clogging model described in Section 3.2.1 and compared our predicted results for the pressures with those measured at the inlet of the capsules 1–5, 7–10 and at the outlet of the top and bottom capsule, both for the co-current and counter-current configuration. In order to assess the quality of our predictions, we plot for a given throughput the maximum absolute error, that is, the maximum absolute error between any of the predicted and measured pressures and the mean error. This is defined as the mean over all absolute errors between the predicted and measured pressures and is very similar to the median error.

The results of the simulation for the counter-current configuration are depicted in Fig. 4. The predicted pressure rises gradually at the beginning before rising rapidly towards the end. The model accurately predicts the measured pressures; the spikes in the error measurements are due to the spikes in the clogging data (Fig. 3a).

The results for the co-current configuration (Fig. 5) show a similar gradual rise at the beginning before the rapid rise at the end; the maximum and mean error for the predictions are better than those for the counter-current configuration.

4. Insights and predictions from the model

In this section, we will show that our model can be used to obtain insights about the flow distribution within a multi-capsule depth filter during a filtration run and how the performance of such a multi-capsule depth filter can be predicted using data from only a few experiments.

4.1. Calculating the normalized differential pressure

An important concept for multi-capsule depth filters is the normalized differential pressure (NDP), which is computed by dividing the pressure difference across a given capsule by the pressure difference across the first capsule from the bottom. In the case where the permeability of each capsule is the same, it indicates the volume of fluid that is processed by each capsule relative to the first capsule. An NDP close to 1 for all capsules is desirable, signifying a homogeneous usage of the processing capacity.

To compute the NDP, Collins et al. [5] used a linear interpolation between the pressure at the bottom and top outlet of the stack in order to estimate the pressure at the outlet of the other capsules. Thus their calculated values of the NDP differ from the actual

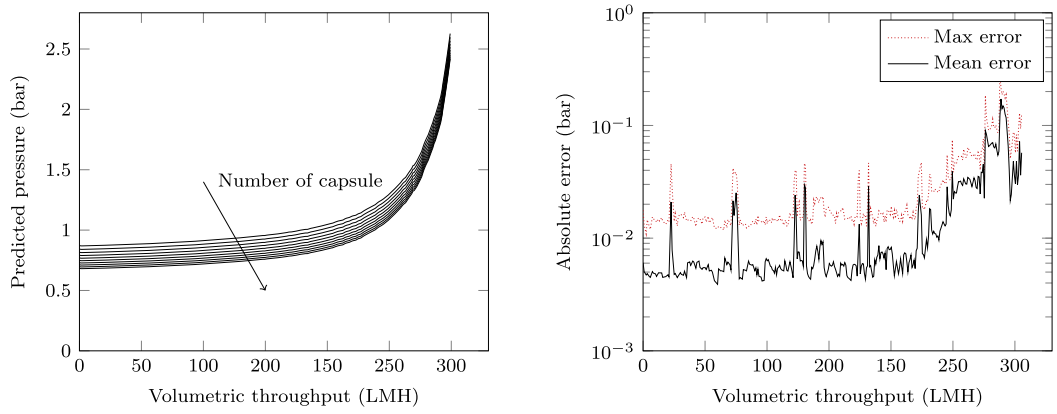

(a) Prediction for a ten-capsule counter-current depth filter, the curves correspond to filters 1 to 10 from top to bottom

(b) Maximum and mean absolute error between the predicted and measured pressures for all capsules

Fig. 4. Predicted pressures at the measuring point and the corresponding prediction errors. We display the maximum absolute and the mean error only for greater clarity.

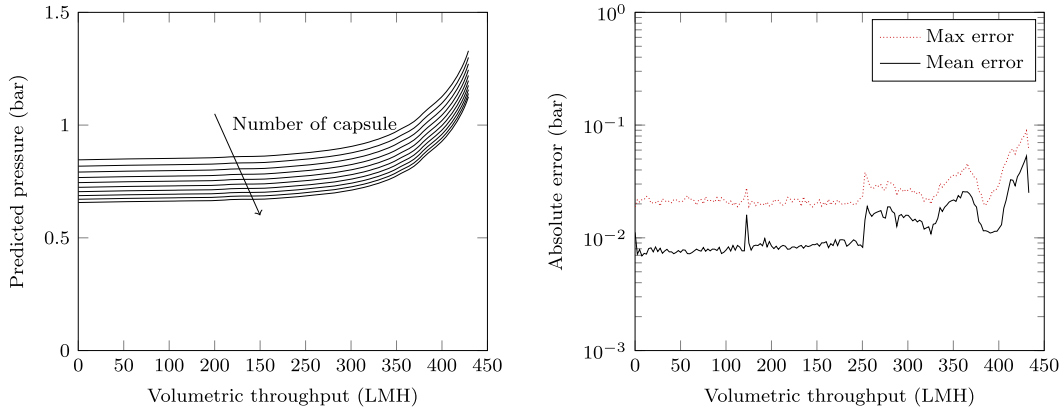

(a) Prediction for a ten-capsule co-current depth filter, the curves correspond to filters 1 to 10 from top to bottom

(b) Maximum and mean absolute error between the predicted and measured pressures for all capsules

Fig. 5. Predicted pressures at the measuring point and the corresponding prediction errors. We display the maximum absolute and the mean error only for greater clarity.

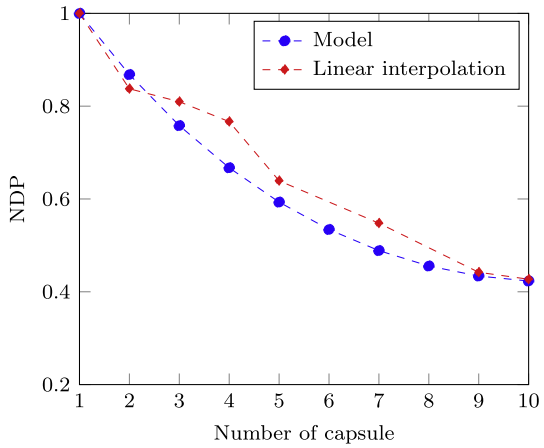

Fig. 6. Comparison of the predicted normalized differential pressure (NDP) based on a linear interpolation and our model for ten capsules in counter-current configuration.

NDP we obtain based on our model, as can be seen in Fig. 6. We use the instance of ten capsules in a counter-current configuration for illustration, although the results in other configurations are similar.

Since the pressure differences between the outlets are uniform, the linear interpolation tends to overestimate the NDP for capsules further up in the stack.

4.2. Predicting the NDP for a multi-capsule depth filter with an arbitrary number of capsules

The predicted NDP in our mathematical model depends only on the parameters for the pressure loss due to friction in the pipe, $r_{i,\text{in}}$, $r_{i,\text{out}}$, and the Darcy parameters α_i of the capsules. If the same capsules are used within the stack, we need only the three parameters r_{in}, r_{out} and α to predict the pressure distribution within a multi-capsule depth filter of any given number of capsules. Furthermore, if we also know the clogging behavior of a single capsule, we can also predict the performance of a multi-capsule depth filter during an entire filtration run to with high accuracy.

As a strategy to precisely predict the filtration capacity of a multi-capsule depth filter, one would conduct clean water flow tests with a multi-capsule depth filter with two capsules to obtain the parameters r_{in}, r_{out} and α. To account for the difference in viscosity between the feed used in the experiment and water, the parameters r_{in}, r_{out} and α would have to be multiplied by the ratio of the water viscosity and the feed viscosity, $\mu_{\text{water}}/\mu_{\text{feed}}$. Finally, one can account for modeling the change in permeability due to clogging as described in Section 3.2.1.

To illustrate the idea of predicting the capacity of a multi-capsule depth filter based on the parameters r_{in}, r_{out} and α, we used the values obtained by the measurements for the five-capsule depth filters to predict the NDP for ten-capsule depth filters. The results for the co-current configuration are shown in Fig. 7 and show a very good agreement, the results for the counter-current configuration are similar but not shown here.

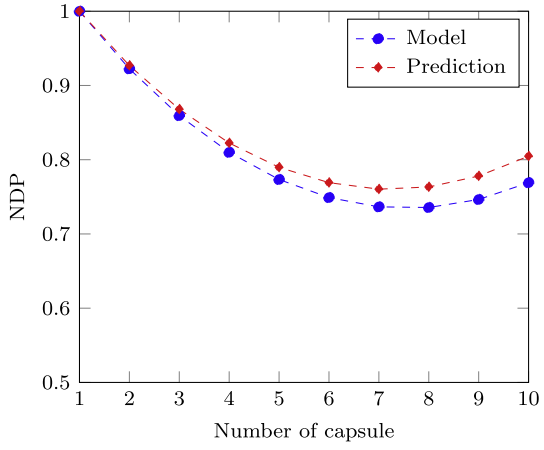

Fig. 7. Comparison of the predicted normalized differential pressure (NDP) across the capsules against the measured NDP in the experiments for a ten-capsule co-current depth filter.

5. Conclusion

In this paper, we derived a system of linear equations describing the flow and pressure distribution within a multi-capsule depth filter based on Darcy's law and the assumption of laminar flow. The corresponding system is dependent on three parameters, corresponding to measures of the resistance of the filter and the resistance in the pipes before and after the filter, which can be inferred from a clean-water flow test in any given multi-capsule depth filter and can then be used to predict the flow and pressure distribution for multi-capsule depth filters with any given number of capsules in a clean-water flow test. The predictions presented in this paper are in good accordance with experimental data.

We then combined this model with fouling data from experiments to derive a numerical method that simulates an entire filtration run. Again, the predictions were in good accordance with the experimental data.

The methods outlined in this paper can be applied to a wide range of scaling-up problems in dead-end filtration systems where filters are used in parallel but can also be extended to cope with filters being connected in series. The method of combining experimental measurements with a model can also be adapted to any filtration system with multiple connected filters to describe their performance during an entire filtration run, provided the key assumption, that the permeability of a given capsule only depends on its throughput, is satisfied. This method has the advantage of delivering highly accurate results while freeing the experimentalist of having to approximate the observed clogging behavior using models.

A patent application concerning the methods described in this paper has been filed [14].

Acknowledgements

A.U.K. is grateful for funding from Pall Corporation and the Mathematical Institute, University of Oxford. I.M.G. gratefully acknowledges support from the Royal Society through a University Research Fellowship.

Appendix A. Existence and uniqueness of the solution

To prove that the solution to the model for N capsules, introduced in Section 2.2, exists and is unique, it is sufficient to work with the hydrodynamic part only. Motivated by their physical meaning, one then continues to assume that all parameters $r_{i,\text{in}}$, $r_{i,\text{out}}$ and α_i are non-zero and have the same sign.

To show uniqueness, assume that the model has two solutions $\mathbf{Q}_a = (Q_1^a, \ldots, Q_N^a)$ and $\mathbf{Q}_b = (Q_1^b, \ldots, Q_N^b)$ and then show that the non-zero residual flux $\mathbf{Q}_a - \mathbf{Q}_b$ violates the assumption that all parameters $r_{i,\text{in}}$, $r_{i,\text{out}}$ and α_i are non-zero and have the same sign.

To prove existence, note that the dimension of the corresponding matrix of the linear system is $2N+2$, the dimension of the image is $2N+2$, and thus, as the dimension of the kernel is $\mathbf{0}$. Existence follows.

Appendix B. Computing the parameters from the experiments

Due to the usage of the same type of capsules, which also corresponds to the connecting pipes having the same geometry, we will work with the assumption that the permeabilities of the membranes are the same. Hence, $\alpha_1 = \cdots = \alpha_N$, $r_{1,\text{in}} = \cdots = r_{N-1,\text{in}}$ and $r_{1,\text{out}} = \cdots = r_{N-1,\text{out}}$. In order to compute the values, we define the function

$$\boldsymbol{F}(\alpha, r_{\text{in}}, r_{\text{out}}) = (\boldsymbol{P}_{\text{in}}, \boldsymbol{P}_{\text{out}}) \tag{B.1}$$

where $\boldsymbol{P}_{\text{in}}$, $\boldsymbol{P}_{\text{out}}$ are the solutions to the linear system arising from Eqs. (5)–(12), as described in Section 2.2, subject to the inlet and outlet pressures being given. We also define Q as the flux through the system based on $\boldsymbol{P}_{\text{in}}$, $\boldsymbol{P}_{\text{out}}$ and α being known. Let $\boldsymbol{M}$ denote the vector with the measurements.

We then compute the parameters by minimizing the functional

$$G := \|\boldsymbol{F} - \boldsymbol{M}\|^2 + |Q - Q_0|^2 \tag{B.2}$$

using techniques from nonlinear least squares approximation. Here, Q_0 denotes some reference flux to uniquely define the solution of the minimization problem.

References

[1] M.A. Cacciuttolo, E. Shane, C. Oliver, E. Tsao, Scale-up considerations for biotechnology-derived products, in: M. Levin (Ed.), Pharmaceutical Process Scale-Up, Drugs and the Pharmaceutical Sciences, Taylor & Francis, 2001 (chapter 4).
[2] P. Ball, Scale-up and scale-down of membrane-based separation processes, Memb. Tech. 2000 (117) (2000) 10–13.
[3] M.E. Laska, R.P. Brooks, M. Gayton, N.S. Pujar, Robust scale-up of dead end filtration: impact of filter fouling mechanisms and flow distribution, Biotechnol. Bioeng. 92 (3) (2005) 308–320.
[4] M. Zlokarnik, Dimensional analysis and scale-up in theory and industrial application, in: M. Levin (Ed.), Pharmaceutical Process Scale-Up, Drugs and the Pharmaceutical Sciences, Taylor & Francis, 2001 (chapter 1).
[5] M. Collins, H. Lari, S. Anderson, R. Leibnitz, A. Kumar, R. Kuriyel, Investigating flow distribution and its effects on scale-up, BioProcess Int. (October) (2009) 46–51.
[6] J. Hermia, Constant pressure blocking filtration laws – application to power-law Non-Newtonian fluids, Trans. Inst. Chem. Eng. 60 (1982) 183–187.
[7] P. Rajniak, S.C. Tsinontides, D. Pham, W.A. Hunke, S.D. Reynolds, R.T. Chern, Sterilizing filtrationprinciples and practice for successful scale-up to manufacturing, J. Memb. Sci. 325 (1) (2008) 223–237.
[8] C. Duclos-Orsello, W. Li, C.-C. Ho, A three mechanism model to describe fouling of microfiltration membranes, J. Memb. Sci. 280 (1-2) (2006) 856–866.
[9] I.M. Griffiths, A. Kumar, P.S. Stewart, A combined network model for membrane fouling, J. Colloid Interface Sci. 432 (0) (2014) 10–18.
[10] S. Ripperger, W. Gösele, C. Alt, T. Loewe, Filtration, 1. Fundamentals, Wiley-VCH Verlag GmbH & Co. KGaA, 2000.
[11] C. Charcosset, Membrane processes in biotechnology: an overview, Biotechnol. Adv. 24 (5) (2006) 482–492.
[12] R. van Reis, A. Zydney, Membrane separations in biotechnology, Curr. Opin. Biotechnol. 12 (2) (2001) 208–211.
[13] R. van Reis, A. Zydney, Bioprocess membrane technology, J. Memb. Sci. 297 (12) (2007) 16–50.
[14] I.M. Griffiths, A.U. Krupp, C.P. Please, Method and system for designing a multi-capsule filter, Patent Application Number 1514003.1, 2015.